Selvadurai, A. P. S. & Najari, M. (2015). *Géotechnique* **65**, No. 2, 126–134 [http://dx.doi.org/10.1680/geot.14.P.174]

Laboratory-scale hydraulic pulse testing: influence of air fraction in cavity on estimation of permeability

A. P. S. SELVADURAI* and M. NAJARI*

When performing transient hydraulic pulse tests on porous materials in the laboratory it is implicitly assumed that the accessible pore space of a porous medium and the pressurised fluid-filled cavity are completely saturated with the permeating fluid. In certain instances the pressurised fluid cavity in a hydraulic pulse test can contain an air fraction introduced through either the experimental procedure or released from the unsaturated regions of the porous medium. The purpose of this paper is to examine the influence of an air fraction within the pressurised region, on the estimation of permeability derived from transient hydraulic pulse tests. A series of hydraulic pulse tests conducted on Stanstead Granite was used to estimate the permeability of the rock. It is shown that if the effect of the cavity air fraction is omitted from the analysis of the hydraulic pulse test, the permeability can be underestimated. The paper also presents a discussion of the potential role the air fraction can contribute to discrepancies in the permeabilities estimated from steady-state tests and hydraulic pulse tests.

KEYWORDS: groundwater; laboratory tests; numerical modelling; permeability

INTRODUCTION

Measurement of permeability characteristics of low-permeability materials including rocks, clays and clay shales forms an important branch of geotechnical experimentation both in the laboratory and in situ. Of particular interest to the present paper are studies that investigate the flow aspects in soils where the permeating fluid can contain gases (Wheeler, 1988; Sills *et al.*, 1991; Sills & Gonzalez, 2001). The thermo-hydraulic behaviour of low-permeability clayey rocks has been investigated in an informative study by Munoz *et al.* (2009), which examines the pore pressure rise in a fluid-filled heated cavity in Opalinus Clay. Although the estimation of in-situ permeability of geologic media is important to the development of reliable solutions relevant to geoenvironmental applications, the laboratory estimation of permeability provides a useful benchmark for preliminary feasibility assessments of complex geoenvironmental solutions. Laboratory estimation of permeability can be carried out using either steady-state or transient techniques on either cylindrical cores recovered from site investigations or block samples recovered from trial pits. The literature in this area is vast and references to important advances in this area can be found in the recent articles by Selvadurai (2007, 2009) and Selvadurai & Selvadurai (2010).

Porous geomaterials often have directional properties that result from the combination of geologic deposition and geostatic stresses that lead to anisotropy in the permeability characteristics. The laboratory and field estimation of the permeability characteristics of anisotropic media is a complex task and experimental techniques tend to focus on the estimation of the principal permeability characteristics that are identifiable by geologic observations of stratification. In general, the estimation of permeability characteristics of crystalline rocks such as granite is made with the assumption that the permeability of the geologic material is isotropic. In practical applications, unless the stratified geologic medium exhibits distinct differences in the principal permeabilities (>10), the medium can be represented by an equivalent isotropic medium where the effective permeability is represented by the geometric mean. In this paper, attention is focused on the relatively isotropic granitic rock that was used in the experimental investigations. The techniques used for the laboratory estimation of permeability largely depend on the range of permeability. Steady-state tests are used when steady flow rates can be established within a reasonable time frame; for example, when tests are conducted on rocks with permeabilities in the range 10^{-14}–10^{-18} m^2 (see e.g. Heystee & Roegiers, 1981; Tidwell & Wilson, 1997; Selvadurai, 2010; Selvadurai & Selvadurai, 2010). The procedure for estimating the permeability from steady-state tests is very straightforward and requires only the solution of Laplace's equation associated with the relevant experimental configuration, that is, the steady flow rate, the boundary potentials and the geometry of the flow domain. Transient tests, which are referred to as hydraulic pulse tests, are usually associated with rocks that have low permeabilities (e.g. for rocks with permeabilities lower than 10^{-18} m^2); in these cases the establishment of a steady state of fluid flow takes an unduly long time and the flow rate cannot be measured accurately. The transient laboratory techniques used to estimate permeability were pioneered by Brace *et al.* (1968) (see also Black & Kipp, 1981; Hsieh *et al.*, 1981; Neuzil *et al.*, 1981; Morin & Olsen, 1987). References to other developments in this area are given by Selvadurai & Carnaffan (1997), Selvadurai *et al.* (2005) and Selvadurai (2009). Estimating permeability of a porous medium from transient hydraulic pulse tests is, however, complicated by the fact that additional information about the medium being tested as well as information relating to the experimental configuration is required; in the conventional 'piezo conduction equation'-based approach, the values of the compressibilities of the pore fluid, the solid grains and the porous skeleton, as well as the porosity of the porous medium are needed. This entails the measurement of additional properties of the porous medium; errors in these measurements them-

Manuscript received 3 September 2014; revised manuscript accepted 19 December 2014.
Discussion on this paper closes on 1 July 2015, for further details see p. ii.
* Department of Civil Engineering and Applied Mechanics, McGill University, Montréal, QC, Canada.

selves can lead to incorrect estimates of the permeability of the porous medium. The piezo-conduction equation-based interpretation of the hydraulic pulse test can be improved by replacing the analysis of the test by appeal to the classical theory of poroelasticity (Biot, 1941; Selvadurai & Yue, 1994; Selvadurai, 1996; Selvadurai & Suvorov, 2012, 2014); however, this can also lead to differences in the estimated permeability (Adachi & Detournay, 1997; Hart & Wang, 1998; Wang, 2000; Selvadurai & Najari, 2013).

The hydraulic pulse testing technique involves the pressurisation of a fluid volume that is connected to the porous medium and allowed to permeate the saturated pore space through a boundary region of the porous medium. As the fluid in the pressurised region migrates through the porous medium, the fluid pressure in the pressurised region is reduced; the decay pattern in the fluid pressure is used to estimate the permeability of the porous medium. When performing an analysis of the hydraulic pulse test, it is implicitly assumed that both the fluid in the pressurised region and the fluid in the pore space of the rock are saturated by a pore fluid void of air. Air in the pressurised fluid can alter its compressibility, which can lead to incorrect estimates of the laboratory permeability characteristics. In a laboratory context, steps can be taken to minimise the influence of air in the pressurised fluid region, but its presence cannot be completely eliminated. The presence of air in fluids that are classified as 'gassy' can influence the attainment of steady flow rates in steady-state tests (Selvadurai, 2009). The presence of a small fraction of air can change the compressibility of the pressurised fluid, which in turn can influence the interpretation of the permeability from hydraulic pulse tests. Studies by Schuurman (1966), Fredlund (1976), Teunissen (1982), Pietruszczak & Pande (1996) and Selvadurai & Ichikawa (2013) have addressed the issue of compressibilities of pore fluids containing air. The objective of this paper is to examine the influence of the air fraction on the compressibility of water, and to examine systematically, using theoretical concepts and experiments conducted on granite, the role of the air void fraction in the pressurised fluid volume on the estimation of permeability from hydraulic pulse tests.

GOVERNING EQUATIONS

Biot's theory of poroelasticity (Biot, 1941) takes into account the coupling between pore fluid pressure, deformations of the porous skeleton and the grains composing the porous medium. The piezo-conduction equation is based on a simplified version of the hydro-mechanical coupling where the time-dependent variations in the skeletal mean stresses are ignored. The partial differential equation governing the time-dependent flow of a compressible pore fluid through the accessible pore space of a deformable medium, consisting of a compressible porous skeleton and compressible grains, reduces to the piezo-conduction equation (Brace *et al.*, 1968), which takes the form

$$\frac{\tilde{K}}{\mu}\nabla^2 p - S_\sigma \frac{\partial p}{\partial t} = 0 \tag{1}$$

where p is the pore fluid pressure, $\tilde{K}$ is the permeability and μ is the dynamic viscosity of the fluid. In equation (1), S_σ is the specific storage defined by

$$S_\sigma = [nC_w + C_{eff} - (n+1)C_s] \tag{2}$$

where n is the porosity, C_w is the compressibility of the pore fluid, C_{eff} (i.e. the inverse of bulk modulus) is the compressibility of the porous skeleton and C_s is the compressibility of the solid grains. Hart & Wang (1998) and Selvadurai & Najari (2013) compared the one-dimensional responses (axially and radially symmetric) in hydraulic pulse tests based on Biot's formulation that considered the full hydromechanical coupling, with results obtained using the reduced approach based on the piezo-conduction equation. These studies showed that the piezo-conduction equation approach, which considers the compressibilities of the permeating fluid, the porous skeleton and the solid grains, can be used for the interpretation of hydraulic pulse test results with negligible error.

Using experimental configurations presented later, here attention is restricted to hydraulic pulse tests that pressurise a fluid-filled cavity at the surface of a fluid-saturated porous medium. Fig. 1 shows a schematic view of the semi-infinite porous medium containing a pressurised fluid-filled cavity that is sealed at the surface by an immovable cap. The cavity region is denoted by Ω and the boundary surface of the cavity is denoted by S. During a hydraulic pulse test, the fluid cavity is subjected to an instantaneous pressure increase, which is denoted by $\bar{p}_0$. The boundary conditions of the pressure decay of the sealed fluid-filled cavity can be written as

$$p(\Omega, t) = \bar{p}(t); \qquad p(\Omega, 0) = \bar{p}(0) = \bar{p}_0 \tag{3}$$

$$\int_S \frac{\tilde{K}}{\mu}\nabla p \cdot \boldsymbol{n}\, \mathrm{d}S = \left(\Omega C_{eq}\frac{\partial p}{\partial t}\right)_\Omega \tag{4}$$

where $\bar{p}(t)$ is the pressure field within the cavity; the pressure field within the porous medium should exhibit the regularity conditions applicable to parabolic partial differential equations with diffusive phenomena (Selvadurai, 2000). Also, C_{eq} is the compressibility of the fluid within the cavity. For example, for completely de-aired water, the compressibility of the fluid within the cavity is approximately $4{\cdot}54 \times 10^{-10}\ \mathrm{Pa}^{-1}$ (White, 1986) and the presence of air can alter this value. The initial condition applicable to the problem is

$$p(\boldsymbol{x}, 0) = 0 \tag{5}$$

where $\boldsymbol{x}$ is the position vector in the porous domain.

Air in water can exist in either a dissolved or gaseous form. Assuming that the air inclusions in the water are in the form of bubbles and neglecting the effects of (*a*) solubility of air in water, (*b*) surface tension of the water and (*c*) the vapour pressure within the bubbles, the compressibility of the air–water mixture can be estimated. Consider a total volume of the mixture (V_t) composed of pure water (V_w) and an air bubble fraction (V_a). The air fraction ϕ is defined as

$$\phi = \frac{V_a}{V_w + V_a} \tag{6}$$

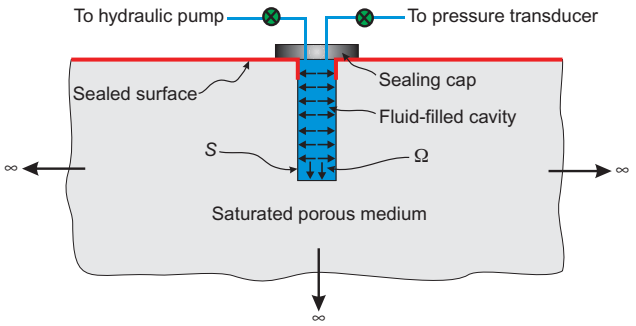

Fig. 1. Hydraulic pulse testing on a semi-infinite porous medium containing a pressurised, sealed fluid cavity

The isothermal compressibilities of the mixture, the pure water and the air, respectively, are

$$C_{eq} = -\frac{dV_t/V_t}{dp}; \quad C_w = -\frac{dV_w/V_w}{dp}; \quad C_a = -\frac{dV_a/V_a}{dp} \tag{7}$$

where dp is an increment of pressure, which is assumed to be identical in all the phases. Substituting $V_t = V_w + V_a$ in the compressibility equation of the mixture (i.e. equation (7)) gives

$$C_{eq} = -\frac{dV_t/V_t}{dp} = -\frac{dV_w/(V_w + V_a)}{dp} - \frac{dV_a/(V_w + V_a)}{dp} \tag{8}$$

The two terms on the right-hand side of equation (8) can be re-written in the form of C_a and C_w

$$\frac{1}{V_a + V_w}\frac{dV_a}{dp} = \phi\frac{1}{V_a}\frac{dV_a}{dp} = \phi C_a; \quad \frac{1}{V_a + V_w}\frac{dV_w}{dp} = (1-\phi)\frac{dV_w}{dp} = (1-\phi)C_w \tag{9}$$

and, upon substituting equation (9) into equation (8), the following is obtained

$$C_{eq} = \phi C_a + (1-\phi)C_w \tag{10}$$

which is the upper bound Voigt estimate (Christensen, 1979; Nguyen & Selvadurai, 1995; Selvadurai & Ichikawa, 2013). Equation (10) gives the compressibility of a fluid–gas mixture with free air bubbles. The compressibility of air can be derived by considering the incremental variations to Boyle's Law for isothermal processes; that is

$$PV_a = \text{const.}; \quad PdV_a + V_a dP = 0 \Rightarrow C_a = \frac{-dV_a/V_a}{dP} = \frac{1}{P} \tag{11}$$

where P is the absolute air pressure.

Boyle's law also determines the changes in the volume of air with pressure. Assuming that the volume of the cavity Ω that is pressurised (i.e. $V_w + V_a$) remains constant during the pulse tests, the air fraction equation can be re-written as

$$P^0V_a^0 = PV_a;\ \phi = \frac{V_a}{V_w + V_a} \Rightarrow \phi = \frac{\frac{P^0}{P}V_a^0}{V_w + V_a} = \frac{P^0}{P}\phi^0 \tag{12}$$

where P^0 is the initial absolute air pressure, V_a^0 is the initial volume of air and ϕ^0 is the initial air fraction in the cavity. Since the effects of surface tension of the water and the vapour pressure within the air bubbles are neglected, the absolute air pressure at any time is equal to the absolute water pressure. Fig. 2 shows the influence of the air fraction, in the form of air bubbles, on the compressibility of the air–water mixture.

From Fig. 2 it can be seen that the amount of air inclusion has a significant effect on the compressibility of the mixture. For instance, for an air fraction of 1%, the compressibility can vary from 1×10^{-9} (Pa^{-1}) to 1×10^{-7} (Pa^{-1}) over a pressure range of 1 MPa. Therefore, depending on the pressure range of interest, air voids can alter the compressibility of the fluid in the pressurised region. The influence of the air fraction in water on its compressibility has also been noted by other researchers, including Schuurman (1966), Fredlund (1976) and Teunissen (1982).

Air can dissolve in water without any chemical interaction and occupy a certain volume of the water. This volume is only temperature-dependent; Henry's law states that the weight of gas dissolved in a certain quantity of liquid at a constant temperature is directly proportional to the pressure of the gas above the solution pressure. Also, Fick's law can be used to describe the rate at which air goes into solution. In this study, however, the role of diffusive transport is not considered. Based on Henry's law, the maximum volume fraction of air in solution is $h(1-\phi)$, where h is Henry's constant and ϕ is the air fraction. Thus, in order to take into account the effect of gas solubility on the compressibility of the gas–fluid mixture, equation (10) is modified as follows

$$C_{eq} = \frac{\phi + h(1-\phi)}{P} + (1-\phi)C_w \tag{13}$$

The dissolved air fraction in equation (13) can contribute to the change in the compressibility of the air–water mixture only if the rate of dissolution of air in the water is comparable to the absolute pressure change in the system. Otherwise, the effect can be neglected. Henry's constant (h) for air at a temperature of 25°C and atmospheric pressure is 0·01708. It should also be noted that, as the volume fraction ϕ increases (>0·05) the compressibility of the mixture that incorporates solubility approaches the estimate for compressibility of a system that excludes solubility (Schuurman, 1966).

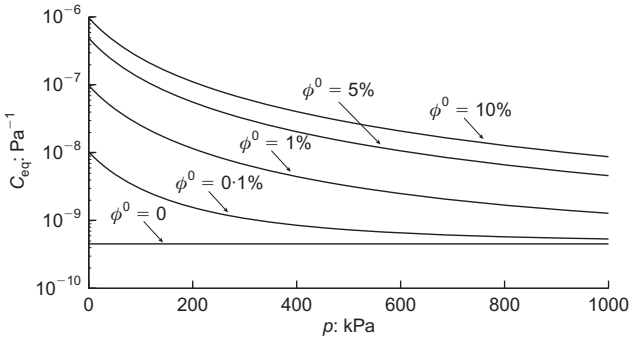

Fig. 2. Compressibility of air–water mixtures with different air fractions

COMPUTATIONAL MODELLING OF THE EFFECT OF AIR INCLUSIONS ON HYDRAULIC PULSE TESTS

In order to examine the influence of an air fraction in the pressurised fluid on the pressure decay that can be observed in a hydraulic pulse test, a typical one-dimensional test configuration was modelled using the multiphysics finite-element code Comsol™. The simulated region measured 100 mm in diameter and 200 mm high. Equations (1) and (2) were used to model the pressure pulse decay process. Fig. 3 shows the geometry and boundary conditions of the problem. The mechanical and physical parameters used in the study were as follows: cross-sectional area of the cylinder (A) = $7{\cdot}85 \times 10^{-3}$ m^2; volume of the pressurised cavity (V_w) = 10^{-5} m^3; porosity (n) = 0·01; compressibility of the porous skeleton (C_{eff}) = $4{\cdot}0 \times 10^{-11}$ Pa^{-1}; Henry's constant (h) = 0; Biot coefficient (α) = 0·44; compressibility of de-aired water (C_w) = $4{\cdot}5 \times 10^{-10}$ Pa^{-1}; dynamic viscosity of water (μ) = 10^{-3} Pa/s; permeability ($\tilde{K}$) = $1{\cdot}0 \times 10^{-18}$ m^2. The fluid-filled cavity was initially pressurised to 100 kPa.

In order to present normalised results for the computational simulation, the time factor T is introduced

$$T = \frac{A^2\tilde{K}t}{\mu V_w^2 C_w} \tag{14}$$

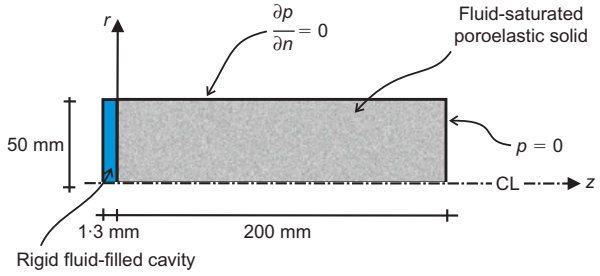

Fig. 3. The geometry and boundary conditions of the one-dimensional hydraulic pulse test

Substituting the values in T gives

$$T = \frac{(7{\cdot}85 \times 10^{-3})^2 \times 1{\cdot}0 \times 10^{-18}}{10^{-3} \times (10^{-5})^2 \times 4{\cdot}54 \times 10^{-10}} t = 1{\cdot}36t$$

where t has units of seconds.

The problem was modelled for different air fractions varying from 0 to 10% and the results for the decay pattern are shown in Fig. 4. It can be observed that the air inclusion in the cavity can significantly affect the interpretation of permeability in hydraulic pulse tests.

Figure 4 shows that there is a significant difference between the hydraulic pressure decay curves for the different air fractions; if the effect of trapped air is not taken into account the interpretation of the permeability parameter from hydraulic pulse tests will be erroneous.

EXPERIMENTAL INVESTIGATION

In order to further examine how any air trapped within the pressurised cavity affects the interpretation of hydraulic pulse test results, experiments were performed on a sample of granite from Stanstead, Quebec. Stanstead Granite is a fine-grained rock; the mechanical and physical properties of the granite have been examined in detail by a number of authors, including Iqbal & Mohanty (2007) and Nasseri *et al.* (2010). Hydraulic pulse tests were performed on a cylindrical sample of Stanstead Granite measuring 49 mm in diameter and 100 mm high and the estimated permeability value was compared with the steady-state test results. The cylinder contained a partially drilled central cavity measuring 7 mm in diameter and 61 mm long, and precautions were taken to minimise damage during coring.

Permeability measurement of the granite sample

To conduct the hydraulic pulse tests, the stainless steel sealing attachment was connected to the cavity using a marine epoxy. This procedure has been used in several previous investigations and the sealing capabilities have been adequately established (Selvadurai & Carnaffan, 1997; Selvadurai *et al.*, 2011; Selvadurai & Jenner, 2012). In order to make the surface of the sample impermeable, the upper surface was coated with the same marine epoxy. The sample prepared for testing is shown in Fig. 5. The cavity pressure was measured using an Omega pressure transducer (range up to 1400 kPa) connected to the fittings. Before performing the experiments, the sample was saturated in a vacuum chamber for 3 days. The central cavity of the sample and the connected fittings were filled with water using a syringe with a hypodermic needle. The total volume of the cavity including the volume of the drilled cavity, the fittings and the pressure transducer, was measured as approximately 10 ml. A schematic view of the experimental arrangement is shown in Fig. 6.

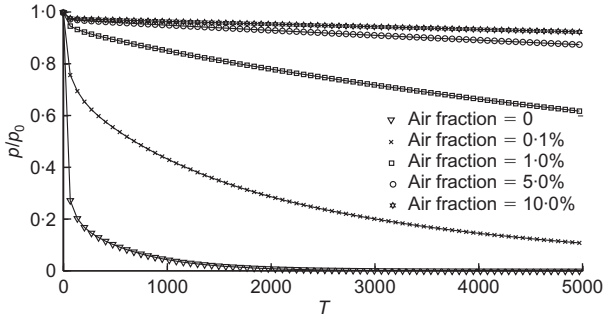

Fig. 4. Effect of air bubbles on cavity pressure decay

Steady-state tests. Initially, the permeability of the Stanstead Granite sample was measured using a steady-state technique under different flow rates (0·0025, 0·005, 0·01 and 0·02 ml/min). Fig. 7 shows the cavity pressure recorded for the different flow rates. The problem was modelled using Comsol Multiphysics™. Table 1 gives the measured steady-state pressure corresponding to each flow rate and the estimated permeability value.

Hydraulic pulse tests. After performing the steady-state tests, a set of hydraulic pulse tests was performed on the same sample. Each test was initiated by pumping water into the sample at a constant flow rate of 2 ml/min. After reaching the desired cavity pressure, the inlet valve was closed and the dissipation of the cavity pressure was monitored. Before the start of each new test, sufficient time (in this case at least 6 h) was allowed for the excess pore pressure generated from the previous test to dissipate. This procedure was adopted (Selvadurai, 2009) in order to eliminate any influence of residual pressures on the interpretation of the hydraulic pulse test results.

Nine hydraulic pulse tests were performed on the sample. The target maximum cavity pressures were 100, 250 and 600 kPa, and three hydraulic pulse tests were performed at each target pressure. The measured cavity pressure changes were then analysed using the Comsol Multiphysics™ software. The piezo-conduction equation was used to model the experiment, taking into account the compressibility of the solid grains. The boundary conditions of the problem are shown in Fig. 8. The parameters used in the analysis were as follows: Young's modulus (E) = 56 GPa, Poisson ratio (ν) = 0·13; porosity (n) = 0·5–1·4%; Biot coefficient (α) = 0·44; compressibility of the fluid (C_w) = $4{\cdot}54 \times 10^{-10}$ Pa^{-1}. The measured cavity pressure curves and the computed bounding decay curves are shown in Fig. 9.

When compared to the steady-state tests, the hydraulic pulse test results showed very low permeability values. The estimated permeability range is one to three orders of

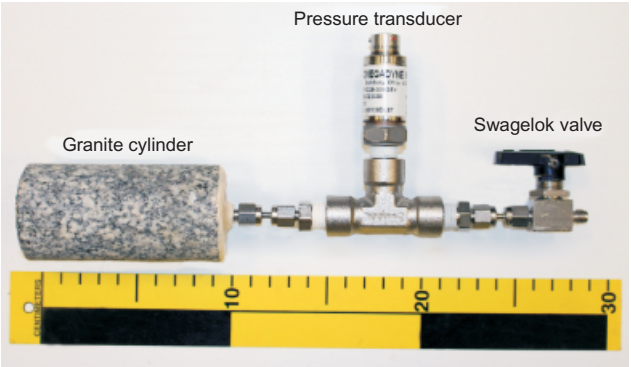

Fig. 5. The assembly of the Stanstead Granite sample

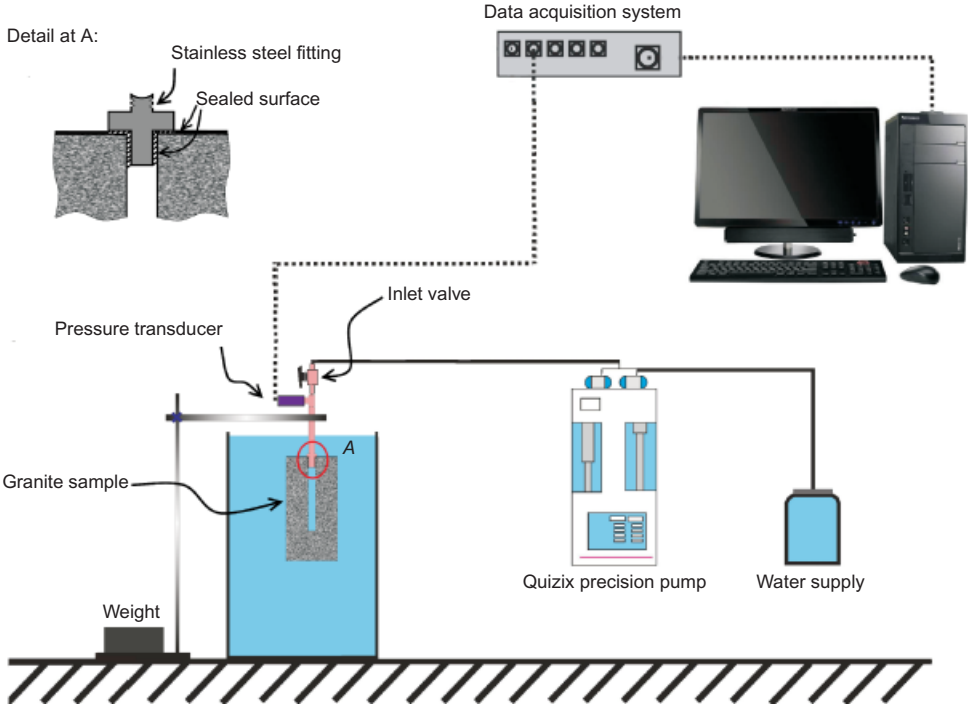

Fig. 6. Schematic view of the hydraulic pulse test experiment performed on the Stanstead Granite sample

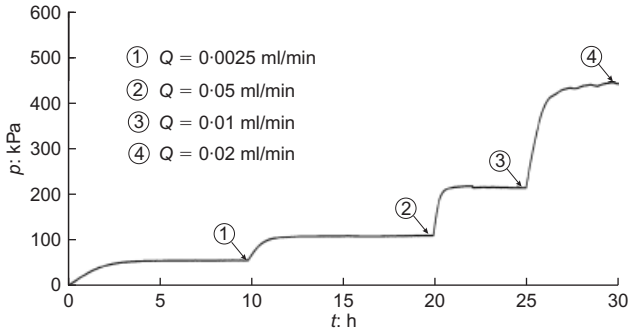

Fig. 7. Changes in cavity pressure for steady-state tests performed on the Stanstead Granite sample at different flow rates

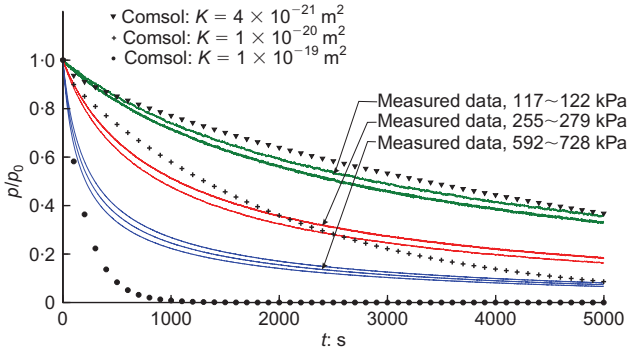

Fig. 9. Hydraulic pulse tests performed on the Stanstead Granite sample compared with results of computational modelling

Table 1. The results of steady-state tests performed on the Stanstead Granite sample

Point	1	2	3	4
Q: ml/min	0·0025	0·005	0·01	0·02
p: kPa	55·1	110	215	433
$\bar{K}$: m^2	$3{\cdot}45 \times 10^{-18}$	$3{\cdot}45 \times 10^{-18}$	$3{\cdot}55 \times 10^{-18}$	$3{\cdot}52 \times 10^{-18}$

magnitude less than the permeability values measured from steady-state experiments. Also, a clear pressure dependency was observed in the measured cavity pressure dissipation curves. Since no pressure dependency was observed in the steady-state experiments, referring to equation (13) it can be concluded that one factor that accounts for the discrepancies could be the existence of air within the pressurised cavity. In order to account for the influence of the compressibility of

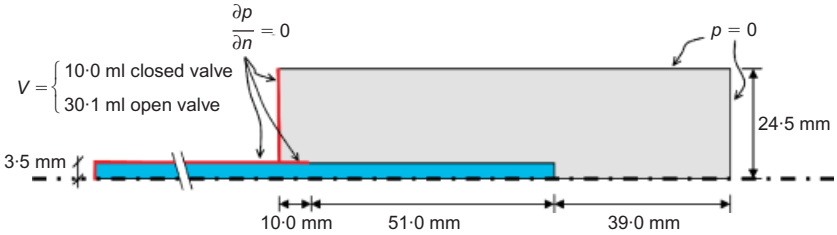

Fig. 8. The geometry and boundary conditions of the Stanstead Granite sample for modelling the hydraulic pulse tests

the air–water mixture in the cavity on the hydraulic pulse tests and to estimate the amount of trapped air in the fluid cavity, it was decided to examine the pressure build-up curves in more detail.

Back-calculation of compressibility change using the experimental results. Assuming that the compressibility of the air–water mixture is C_{eq} and that water is injected into the cavity at a constant flow rate, the time-dependent compressibility of the air–water mixture can be expressed in the form

$$C_{eq} = -\frac{dV_t/V_t}{dp} \Rightarrow C_{eq} = -\frac{1}{V_t}\frac{dV_t/dt}{dp/dt} \quad (15)$$

where V_t is the participating volume at the pressure build-up stage. This volume includes the volume of the rock cavity, the volume of the connection fittings and the volume of the pump cylinder. Using the definition of Q and performing integrations, the following is obtained

$$Q = -\frac{dV_t}{dt};\ V_t(t) = V_t^0 - Qt \quad (16)$$

where V_t^0 is the initial total volume of the cavity. This gives

$$C_{eq} = \frac{1}{V_t^0 - Qt}\frac{Q}{dp/dt} \quad (17)$$

The above equation can be approximated by

$$C_{eq} \approx \frac{Q/(V_t^0 - Qt)}{\Delta p/\Delta t} \quad (18)$$

In order to estimate the variation in the compressibility of the cavity fluid, C_{eq}, for the hydraulic pulse tests performed on the Stanstead Granite sample, the pressure build-up curves recorded in the tests were used along with equation (18). Fig. 10 shows the change of C_{eq} with pressure for the cavity pressure build-up stage of the test. The compressibility of the cavity fluid was $7{\cdot}0 \times 10^{-9}\,Pa^{-1}$ to $3{\cdot}4 \times 10^{-7}\,Pa^{-1}$ for the applied pressure range, which is much higher than the value usually assumed for the parameter. Therefore, the assumption of constant compressibility of de-aired water, $C_w = 4{\cdot}54 \times 10^{-10}$ (Pa^{-1}), is not valid when a large pressure range is encountered, similar to the conditions that can exist within the pressurised cavity.

Figure 11 shows the measured pressure build-up curve. In order to estimate the air fraction trapped in the cavity, the build-up of pressure in the sample was modelled using Comsol Multiphysics™. The parameters used in the model are: $V_0 = 30{\cdot}1$ ml (this includes the volumes of the cavity region, the fittings, the connecting tube and the volume of water in the pump cylinder), $Q = 2$ ml/min, $\tilde{K} = 3 \times 10^{-18}$ to $4 \times 10^{-21}\,m^2$ and $n = 0{\cdot}5$–$1{\cdot}4\%$. The pressure

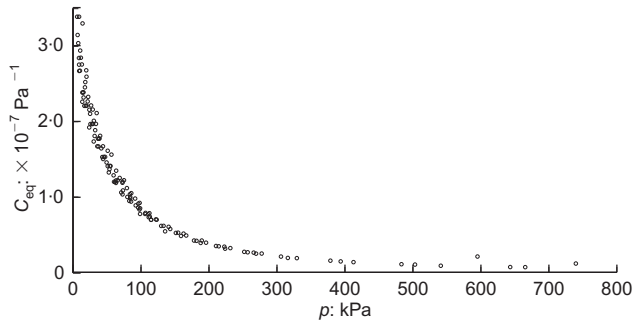

Fig. 10. Change of C_{eq} with cavity pressure increase in Stanstead Granite sample

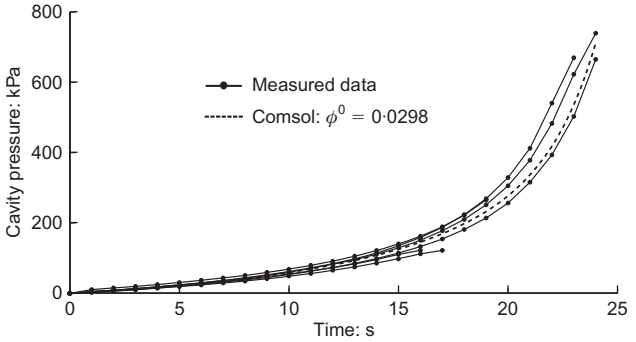

Fig. 11. Experimental results for the build-up of cavity pressure due to pumping water at the rate of $Q = 2$ ml/min, for the Stanstead Granite sample

build-up curves were fitted with the initial air fraction of $\phi^0 = 0{\cdot}0298$. Since the duration of pressure build-up is short, variations in permeability of the rock within the range of 3×10^{-18} to $4 \times 10^{-21}\,m^2$ did not affect the pressure build-up curve. In general, if the volume of water that flows from the rock cavity to the porous medium is negligible during the pressure build-up stage, the rock can be regarded as impervious while the cavity pressurisation is performed. The condition can be satisfied by choosing a high flow rate that minimises the duration of the pressure build-up stage in comparison to the regular hydraulic pressure pulse decay stage.

Estimation of the permeability range. As shown in Fig. 9, the hydraulic decay curves for the pulse tests are dependent on the initial pressure, which cannot be explained by a constant value of C_{eq}. In order to estimate the permeability, the results of hydraulic pulse tests were analysed using the compressibility of the air–water mixture for the cavity fluid. It could be assumed that the accessible pore space in the sample was fully saturated during the vacuum saturation process and hence the compressibility of *de-aired water* was used for modelling the specific storage of the porous medium. The results for the drop in the cavity pressure were examined. The air fraction estimated from the pressure build-up curves was obtained with the assumption that the inlet valve was open, whereas during pressure decay the inlet valve is closed. Hence, in order to estimate the air fraction to be used in the analysis of hydraulic pulse decay curves, it should be modified to account for the reduced volume of the cavity. In the present example, the initial air fraction was estimated for a volume of 30·1 ml, whereas after closing the inlet valve the volume of the fluid cavity in connection with the porous medium reduces to 10 ml. Therefore, with the assumption that the air bubbles are trapped in the fittings ahead of the valve location, the estimated air fraction should be multiplied by (30·1/10). The experiment was modelled in Comsol™ for three different maximum cavity pressures (120, 265 and 660 kPa). The values are the average of the cavity pressures measured in the experiments and the results are shown in Fig. 12.

In practice, with the increase in the cavity pressure the trapped air gets partially dissolved in the water; the dissolution of the air decreases the cavity pressure. A complete model should also take into account the effect of the time and pressure-dependency of air in water. However, the simplified method proposed here provides an acceptable level of accuracy for the estimation of permeability using the hydraulic pulse testing technique. The estimated permeability for the Stanstead Granite sample is $3{\cdot}2 \times 10^{-18}\,m^2$.

Injecting air into the cavity. In order to further investigate the effect of the air content on the hydraulic pressure decay,

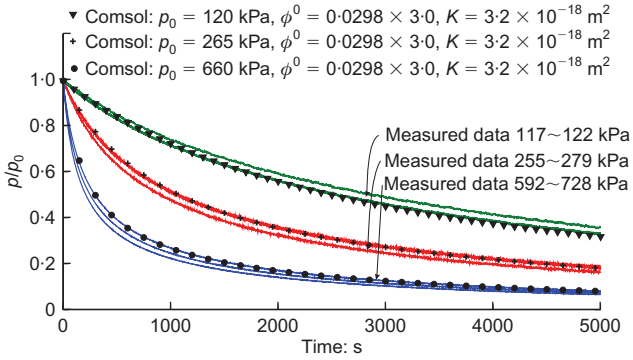

Fig. 12. Hydraulic pulse test results performed on the Stanstead Granite sample compared with results of computational modelling that takes into account the effect of air voids

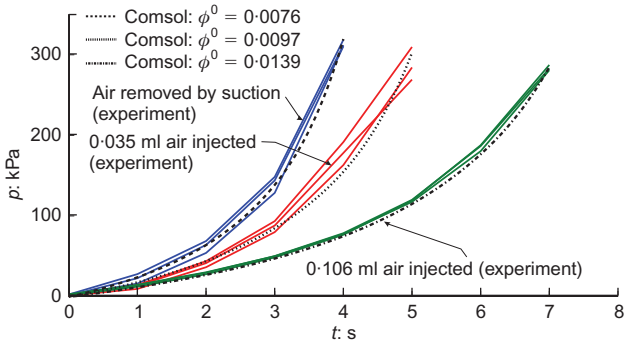

Fig. 13. Experimental results for the build-up of cavity pressure due to pumping water at the rate of $Q = 2$ ml/min, for the three sets of hydraulic pulse tests performed on the Stanstead Granite sample

measured volumes of air were introduced to the fluid-filled cavity of the sample in two steps. The sample was initially immersed in water and the fitting was connected to a Venturi pump that applied suction to the fluid-filled cavity. A transparent plastic pipe was used to connect the vacuum pump to the cavity fitting in order to observe the extracted air bubbles. The applied suction helped to remove the trapped air bubbles from the cavity. The extraction of air bubbles appeared to stop after almost a day of application of the suction; however, the suction was continued for a further 24 h in order to ensure that the extraction of air from the system was complete. The vacuum pump was then turned off and the negative pore pressure in the rock was allowed to dissipate for a day before commencing the hydraulic pulse tests. The experiments were conducted in three steps: (*a*) three hydraulic pulse tests were performed on the sample after removal of the trapped air bubbles by suction; (*b*) three hydraulic pulse tests were performed after purposely introducing 0·035 ml of air into the fluid-filled cavity; and (*c*) three hydraulic pulse tests were conducted after introducing a further 0·106 ml of air into the fluid-filled cavity. (The introduction of air into the cavity cannot be performed in an exact manner and hence the choice of a range of the volumes.)

All of the hydraulic pulse tests commenced by pumping water into the cavity at a constant flow rate of 2 ml/min. When the fluid pressure in the cavity reached 300 kPa, the inlet valve was closed. A syringe with a hypodermic needle was used to remove water from the cavity for steps (*b*) and (*c*). The syringe was weighed before and after removing water from the cavity using a 104-s Mettler Toledo^{TM} measuring scale with an accuracy of 0·1 mg; the difference between the measured weights of the syringe equals the amount of the extracted water. Since the volume of water extracted from the cavity is replaced by air, the calculated weight difference can be associated with the volume of air added to the cavity. Fig. 13 shows the measured pressure build-up curves for the three sets of hydraulic pulse tests.

The curves were fitted using Comsol^{TM}, assuming an air fraction of $\phi^0 = 0{\cdot}0076$ for step (*a*), $\phi^0 = 0{\cdot}0097$ for step (*b*), and $\phi^0 = 0{\cdot}0139$ for step (*c*). The above-mentioned air fractions were then used to back-calculate the volume of trapped air in each step. Using the total cavity volume of 22·3 ml (including the cavity region, the fittings, the volume of water in the connection pipe and the pump cylinder) the air volumes were estimated as 0·169 ml for the suction-saturated state, 0·047 ml for the first injection of air and 0·094 ml for the second injection of air. The estimated injected air volumes compare favourably with the measured volumes.

Figure 14 shows the pressure decay curves for the three

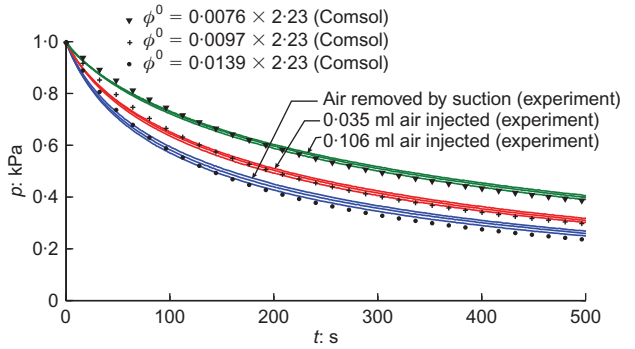

Fig. 14. Hydraulic pulse test results performed on the Stanstead Granite sample with three different air fractions

sets of hydraulic pulse tests performed on the sample. As expected, the cavity pressure decay decreases with the increases in air fraction. The measured fluid pressure curves were then fitted using Comsol^{TM}. A permeability of $3{\cdot}2 \times 10^{-18}$ m^2 is the best fit for the results of the three sets of test for the pressure drop.

CONCLUDING REMARKS

In this paper, a technique is proposed to account for the effects of air that could be present in the cavity region when it is pressurised to perform hydraulic pulse tests. While every precaution is taken to remove air from the pressurised cavity, its presence cannot be completely eliminated, even in experiments conducted in a controlled laboratory environment. The presence of air has a direct influence on the compressibility of the fluid in the pressurised region and its effective compressibility is also influenced by the pressure within the cavity. These effects can contribute to the discrepancies observed in the estimates of permeability derived from steady-state tests and hydraulic pulse tests. While the steady-state tests perhaps give the most accurate estimates of permeability, they are time consuming. Therefore, transient hydraulic pulse tests are advocated in situations where the porous geomaterial is presumed to have low permeability. The influence of the air content on the estimation of permeability is examined using experiments conducted on Stanstead Granite and by computational simulations of the piezo-conduction equation. The paper advocates that both test procedures and computational approaches be used to provide accurate interpretations of hydraulic pulse tests. In this study, however, attention is not focused on the possible migration of the air in the cavity into the fully saturated porous medium. It is implicitly assumed that the air entry

value for the rock is sufficiently small to prevent such processes and that the pressure decay will occur within a time frame that will not result in the migration of the air into the pore space of the rock. The experimental studies were performed at a constant ambient temperature and within the pressure range of 100–600 kPa, which are the common conditions used in most laboratory permeability measurement tests; higher pressures can result in the collapse of air bubbles, which is not examined in this work.

Referring to the hydraulic pulse experiments, by assuming a constant compressibility of $C_w = 4.54 \times 10^{-10}$ Pa^{-1} for pure water within the sealed cavity, the permeability of the Stanstead Granite was estimated to be within the range of 1×10^{-19} to 4×10^{-21} m^2; these results are one to three orders of magnitude different from those obtained from steady-state tests. However, after modifying the compressibility parameters for the tests, the permeability values for the Stanstead Granite obtained from the pulse tests were estimated to be approximately $3{\cdot}2 \times 10^{-18}$ m^2, which is within the same range as the values obtained from the steady-state test results. A set of hydraulic pulse tests was also performed on the sample where measured volumes of air were deliberately injected into the cavity. The experimental cavity pressure curves were then analysed using the suggested technique. The estimated air fractions were very close to the injected values and the technique was successful in estimating the permeability for different air fraction volumes present in the pressurised cavity.

ACKNOWLEDGEMENTS

The work described in this paper was performed at the Environmental Geomechanics Laboratory at McGill University and supported by Discovery and Strategic Research Grants awarded to A. P. S. Selvadurai. The use of the Comsol Multiphysics^{TM} code is for demonstration purposes only and not a statement of endorsement of its use without adequate validation.

NOTATION

C_a	compressibility of air
C_{eff}	compressibility of porous skeleton
C_{eq}	compressibility of fluid within cavity
C_s	compressibility of solid grains
C_w	compressibility of pore fluid
E	Young's modulus
h	Henry's constant
$\tilde{K}$	permeability
n	porosity
$\boldsymbol{n}$	unit normal vector
P	absolute air pressure
P^0	initial absolute air pressure
p	fluid pressure
$\bar{p}_0$	instantaneous pressure increase in cavity region
$\bar{p}(t)$	pressure field within cavity
$p(\Omega, t)$	pressure field within porous medium
Q	pumping flow rate
S	boundary surface of cavity region
S_σ	specific storage
T	normalised time factor
t	elapsed time
V_a	volume of air bubble fraction
V_a^0	initial volume of air
V_t	volume of air–water mixture
V_t^0	initial volume of air–water mixture
V_w	volume of pure water
$\boldsymbol{x}$	position vector
α	Biot's coefficient
μ	dynamic viscosity of water
ν	Poisson ratio
ϕ	air fraction in cavity
ϕ^0	initial air fraction in cavity
Ω	cavity region
∇	gradient operator
∇^2	Laplace operator

REFERENCES

Adachi, J. I. & Detournay, E. (1997). A poroelastic solution of the oscillating pore pressure method to measure permeabilities of 'tight' rocks. *Int. J. Rock Mech. Mining Sci*. **34**, No. 3–4, 062.

Biot, M. A. (1941). General theory of three-dimensional consolidation. *J. Appl. Physics* **12**, No. 2, 155–164.

Black, J. H. & Kipp, K. L. (1981). Determination of hydrogeological parameters using sinusoidal pressure tests: a theoretical appraisal. *Water Resources Res*. **17**, No. 3, 686–692.

Brace, W. F., Walsh, J. B. & Frangos, W. T. (1968). Permeability of granite under high pressure. *J. Geophys. Res*. **73**, No. 6, 2225–2236.

Christensen, R.M. (1979). *Mechanics of composite materials*. New York, NY, USA: Wiley Interscience.

Fredlund, D.G. (1976). Density and compressibility characteristics of air-water mixtures. *Can. Geotech. J.* **13**, No. 4, 386–396.

Hart, D. J. & Wang, H. F. (1998). Poroelastic effects during a laboratory transient pore pressure test. In *Poromechanics* (eds J. F. Thimus, Y. Abousleiman, A. H.-D. Cheng, O. Coussy and E. Detournay), pp. 579–582. Rotterdam, the Netherlands: Balkema.

Heystee, R. & Roegiers, J.-C. (1981). The effect of stress on the primary permeability of rock cores – a facet of hydraulic fracturing. *Can. Geotech. J.* **18**, No. 2, 195–204.

Hsieh, P. A., Tracy, J. V., Neuzil, C. E., Bredehoeft, J. D. & Silliman, S. E. (1981). A transient laboratory method for determining the hydraulic properties of 'tight' rocks – I. Theory. *Int. J. Rock Mech. Mining Sci. Geomech. Abstr.* **18**, No. 3, 245–252.

Iqbal, M. J. & Mohanty, B. (2007). Experimental calibration of ISRM suggested fracture toughness measurement techniques in selected brittle rocks. *Rock Mech. Rock Engng* **40**, No. 5, 453–475.

Morin, R. H. & Olsen, H. W. (1987). Theoretical analysis of the transient pressure response from a constant flow rate hydraulic conductivity test. *Water Resources Res*. **23**, No. 8, 1461–1470.

Munoz, J. J., Alonso, E. E. & Lloret, A. (2009). Thermo-hydraulic characterization of soft rock by means of heating pulse tests. *Géotechnique* **59**, No. 4, 293–306, http://dx.doi.org/10.1680/geot.2009.59.4.293.

Nasseri, M. H. B., Grasselli, G. & Mohanty, B. (2010). Fracture toughness and fracture roughness in anisotropic granitic rocks. *Rock Mech. Rock Engng* **43**, No. 4, 403–415.

Neuzil, C. E., Cooley, C., Silliman, S. E., Bredehoeft, J. D. & Hsieh, P. A. (1981). A transient laboratory method for determining the hydraulic properties of 'tight' rocks -II. Application. *Int. J. Rock Mech. Mining Sci. Geomech. Abstracts* **18**, No. 3, 253–258.

Nguyen, T. S. & Selvadurai, A. P. S. (1995). Coupled thermal-mechanical-hydrological behaviour of sparsely fractured rock: implications for nuclear fuel waste disposal. *Int. J. Rock Mech. Mining Sci. Geomech. Abstr*. **32**, No. 5, 465–479.

Pietruszczak, S. & Pande, G. N. (1996). Constitutive relations for partially saturated soils containing gas inclusions. *J. Geotech. Engng, ASCE* **122**, No. 1, 50–59.

Schuurman, I. E. (1966). The compressibility of an air-water mixture and a theoretical relation between the air and water pressures. *Géotechnique* **16**, No. 4, 269–281, http://dx.doi.org/10.1680/geot.1966.16.4.269.

Selvadurai, A. P. S. (ed.) (1996). *Mechanics of poroelastic media.* Amsterdam, the Netherlands: Kluwer.

Selvadurai, A. P. S. (2000). *Partial differential equations in mechanics. Vol. 1: Fundamentals, Laplace's equation, the diffusion equation, the wave equation*. Berlin, Germany: Springer Verlag.

Selvadurai, A. P. S. (2007). The analytical method in geomechanics. *Appl. Mech. Rev.* **60**, No. 3, 87–106.

Selvadurai, A. P. S. (2009). Influence of residual hydraulic gradients

on decay curves for one-dimensional hydraulic pulse tests. *Geophys. J. Int*. **177**, No. 3, 1357–1365.

Selvadurai, A. P. S. & Carnaffan, P. (1997). A transient pressure pulse method for the measurement of permeability of a cement grout. *Can. J. Civ. Engng* **24**, No. 3, 489–502.

Selvadurai, A. P. S. & Ichikawa, Y. (2013). Some aspects of air-entrainment on decay rates in hydraulic pulse tests. *Engng Geol*. **165**, 38–45.

Selvadurai, A. P. S. & Jenner, L. (2012). Radial flow permeability testing of an argillaceous limestone. *Ground Water* **51**, No. 1, 100–107.

Selvadurai, A. P. S. & Najari, M. (2013). On the interpretation of hydraulic pulse tests on rock specimens. *Adv. Water Resources* **53**, 139–149.

Selvadurai, A. P. S. & Selvadurai, P. A. (2010). Surface permeability tests: experiments and modelling for estimating effective permeability. *Proc. R. Soc. A: Math., Phys., Engng Sci*. **466**, No. 2122, 2819–2846.

Selvadurai, A. P. S. & Suvorov, A. P. (2012). Boundary heating of poroelastic and poro-elastoplastic spheres. *Proc. R. Soc. A: Math., Phys., Engng Sci.* **468**, No. 2145, 2779–2806.

Selvadurai, A. P. S. & Suvorov, A. P. (2014). Thermo-poromechanics of a fluid-filled cavity in a fluid-saturated geomaterial. *Proc. R. Soc. A: Math., Phys., Engng Sci.* **470**, No. 2163, 20130634.

Selvadurai, A. P. S. & Yue, Z. Q. (1994). On the indentation of a poroelastic layer. *Int. J. Numer. Analyt. Methods Geomech.* **18**, No. 3, 161–175.

Selvadurai, A. P. S., Boulon, M. J. & Nguyen, T. S. (2005). The permeability of an intact granite. *Pure Appl. Geophysics* **162**, No. 2, 373–407.

Selvadurai, A. P. S., Letendre, A. & Hekimi, B. (2011). Axial flow hydraulic pulse testing of an argillaceous limestone. *Environ. Earth Sci*. **64**, No. 8, 2047–2058.

Selvadurai, P. A. (2010). *Permeability of Indiana limestone: experiments and theoretical concepts for interpretation of results*. MEng thesis, McGill University, Montreal, Canada.

Sills, G. C. & Gonzalez, R. (2001). Consolidation of naturally gassy soft soil. *Géotechnique* **51**, No. 7, 629–639, http://dx.doi.org/10.1680/geot.2001.51.7.629.

Sills, G. C., Wheeler, J., Thomas, S. D. & Gardner, T. N. (1991). Behaviour of offshore soils containing gas bubbles. *Geotechnique* **41**, No. 2, 227–241, http://dx.doi.org/10.1680/geot.1991.41.2.227.

Teunissen, J. A. M. (1982). Mechanics of a fluid–gas mixture in a porous medium. *Mech. Mater.* **1**, No. 3, 229–237.

Tidwell, V. C. & Wilson, J. L. (1997). Laboratory method for investigating upscaling. *Water Resources Res*. **33**, No. 7, 1607–1616.

Wang, H. F. (2000). *Theory of linear poroelasticity with applications to geomechanics and hydrogeology*. Princeton, NJ, USA: Princeton University Press.

Wheeler, S. J. (1988). A conceptual model for soils containing large gas bubbles. *Géotechnique* **38**, No. 3, 389–397, http://dx.doi.org/10.1680/geot.1988.38.3.389.

White, F. M. (1986). *Fluid mechanics*. Boston, MA, USA: McGraw-Hill.